Electronic Supplementary Material (ESI) for Physical Chemistry Chemical Physics

Supporting Information

Micellar Drug Nanocarriers and Biomembranes: How do they Interact?

Antonio De Nicola,[a,b] *Samira Hezaveh,*[c] *Ying Zhao,*[d] *Toshihiro Kawakatsu,*[e] *Danilo Roccatano,*[c] *and Giuseppe Milano,*[*a,b]

[a]Dipartimento di Chimica e Biologia, Università di Salerno, I-84084 via Ponte don Melillo Fisciano (SA), Italy

[b]IMAST Scarl-Technological District in Polymer and Composite Engineering, P.le Bovio 22, 80133 Napoli (NA), Italy

[c]Jacobs University Bremen, Campus Ring 1, D-28759 Bremen, Germany

[d]Institute of Nano-photonics, School of Physics and Materials Engineering, Dalian Nationalities University, Dalian 116600, China

[e]Department of Physics, Tohoku University, Aoba, Aramaki, Aoba-ku, Sendai 980-8578, Japan

*e-mail: gmilano@unisa.it

Models and parameters

The initial set of χ paramaters for the interaction between polyethylen oxide (EO) and polypropylene oxide (PO) with phospholipid bilayer hase been obtained from a DPD study of Groot[1]. The refinement of these parameters has been based on the reproduction of electron density profile of correspondig atomistic simulations of 1,2-dimethoxyethane (DME) and 1,2-dimetoxypropane (DMP) reported in reference[2]. The electron density profiles reported in **Figure S1** have been calculated averaging on the last 150 ns of each trajectory. The composition of the systems used for the parametrization is reported in **Table 1**. The resulting χ parameters interaction matrix of the CG model are reported in **Table 2**.

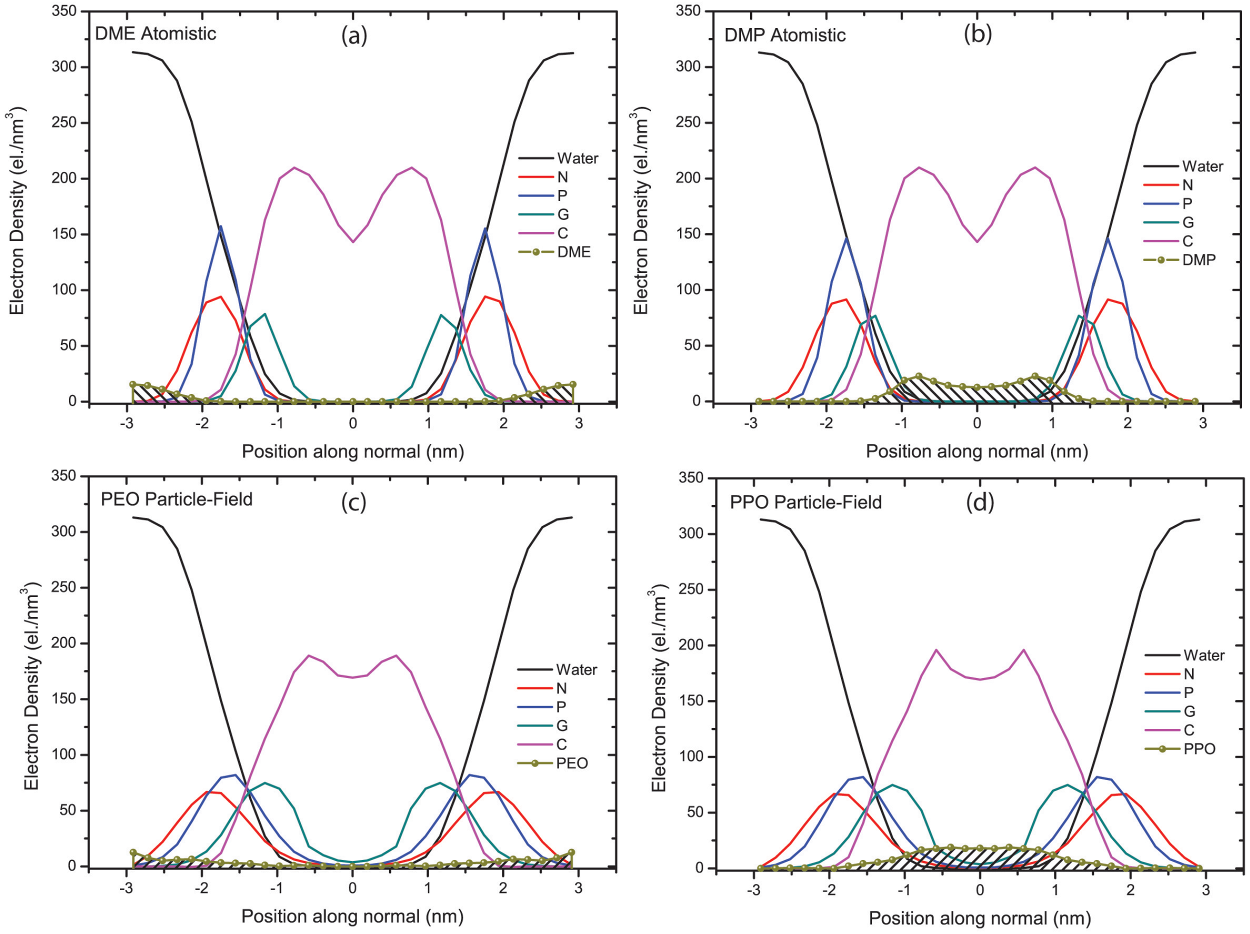

Figure S1 Electron density profiles of : (a) System of 1,2-dimethoxyethane in lipid/water mixture. (b) System of 1,2-dimethoxypropane in lipid/water mixture. (c) Sytem of EO trimers in lipid water mixture. (d) System of PO trimers in lipid/water mixture.

Table 1. Composition of Systems.

System	**Composition (no. Particles)**			**Box size**
	DMPC	Oligomer	no. of Water	(nm)
a	128	1 DME	7962	6.34x6.34x9.69
b	128	1 DMP	7958	6.43x6.43x9.40
c	128	1 PEO	1990*	6.34x6.34x9.69
d	128	1 PPO	1989*	6.43x6.43x9.40

*The values reported as no. of Water are relative to CG water beads. One water bead correspond to four real water molecules.

Table 2. Particle-field interaction matrix. χ_{AB} ×RT(kJ mol^{-1}).

Bead type	**N**	**P**	**G**	**C**	**Water**	**EO**	**PO**
N	0.00	-1.50	6.30	9.0	-8.10	-5.25	2.60
P	-1.50	0.00	4.50	13.50	-3.60	-0.75	7.55
G	6.30	4.50	0.00	6.30	4.50	5.00	0.00
C	9.00	13.50	6.30	0.00	33.75	7.80	-1.60
Water	-8.10	-3.60	4.50	33.75	0.00	1.50	4.60
EO	-5.25	-0.75	5.00	7.89	1.50	0.00	16.00
PO	2.60	7.55	0.00	-1.60	4.60	16.00	0.00

Critical Micelle Concentration (CMC) of Pluronics Model

We investigate the CMC of the model considering the stability of the micelle aggregate as function of the concentration of L64 in water. In particular 5 different concentrations have been considered. The composition of such systems is reported in **Table 3**. For each system we calculate the distribution of free and assembled chains, according to the number of neighbouring chains (zero neighbouring are considered free chains). The number of neighbors is calculated on the basis of cut off criteria (1 nm) on the shorter distance between PO units of two different chains. In **Figure S2** the time behavior of the fraction of assembled L64 chains is reported. We found that the CMC of the proposed model is in an interval ranging from 0.532 to 0.354 mM. This interval is very close to the experimental CMC value of 0.344 mM at 313K reported by Alexandridis[3].

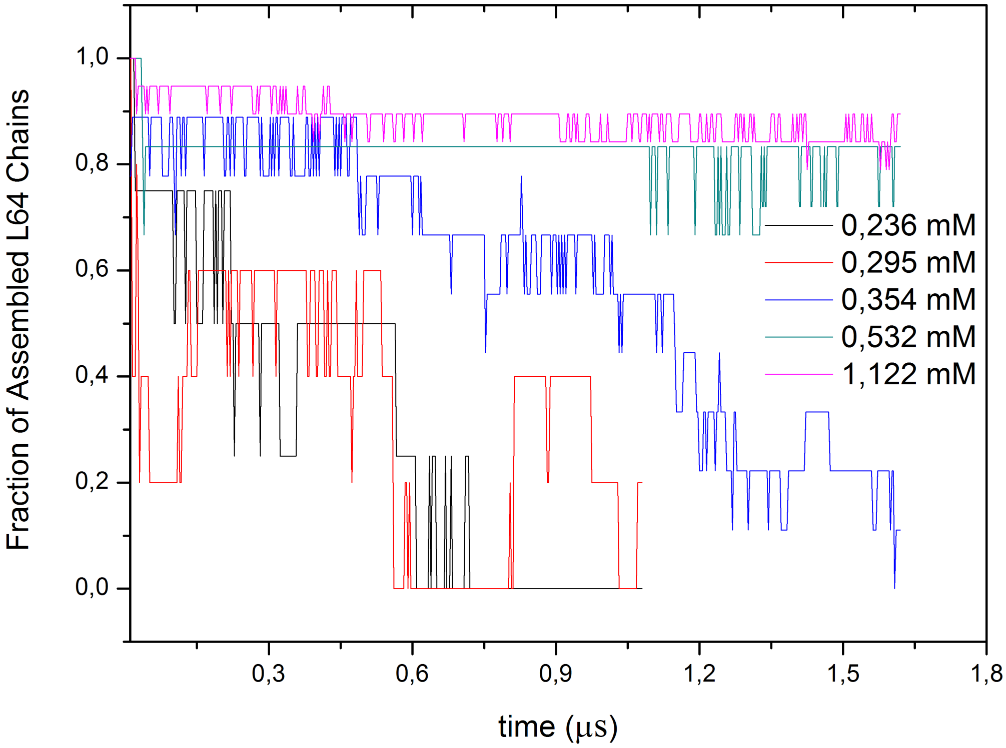

Figure S2 Time behavior of fraction of assembled L64 chains at different concentrations.

Table 3 Composition of systems used for the CMC calculation.

System	**Composition**			**Box Size**	
	no. L64	no. Water	no. Particles	mM	(nm)
A	19	223264	224328	1.122	30.0 x 30.0 x30.0
B	9	223824	224328	0.532	30.0 x 30.0 x 30.0
C	6	223992	224328	0.354	30.0 x 30.0 x 30.0
D	5	224048	224328	0.295	30.0 x 30.0 x 30.0
E	4	224104	224328	0.236	30.0 x 30.0 x 30.0

*The values reported as no. of Water are relative to CG water beads. One water bead correspond to four real water molecules.

Supplementary Results

Aggregation Number

Experimentally the micelle number of aggregation ($N_{\text{agg.}}$) for a system of Pluronic L64 at 2.5 wt% is 38 (at 313 K)[4]. In order to understand the behavior of our model respect to the number of aggregation, we performed 5 simulations (a-e) of a single micelle in water with increasing number of L64 chains, starting from 38 up to 53. Moreover, we fixed the concentration of these systems at 2.5 wt%. The composition of the simulated systems is reported in **Table 4**.

In **Figure S3** we report the occurrence frequency versus the cluster size at different time. The plot in **Figure S3-(a)** is relative to the system of the micelle made by 38 chains of L64. It is clear that $N_{\text{agg.}}$ is strictly close to 38. Increasing the number of L64 chains constituting the micelle, we observe a broader distribution cluster size respect to the reference system (a). In addition, we report in **Figure S4** also the time behavior of cluster size for the systems (a-e).

Table 4 System composition relative at the figure S4.

System	**Composition**				**Box size**	**Simulated time**
	no. of L64	no. of Water	no. Particle	Conc. wt%	(nm)	(μs)
a	38	54733	56861	2.5	18.0x18.0x18.0	4.2
b	41	59095	61391	2.5	18.4x18.4x18.4	4.2
c	45	64861	67381	2.5	18.9x18.9x18.9	4.2
d	48	69185	71873	2.5	19.4x19.4x19.4	4.2
e	53	76444	79359	2.5	20.1x20.1x20.1	4.2

*The values reported as no. of Water are relative to CG water beads. One water bead correspond to four real water molecules.

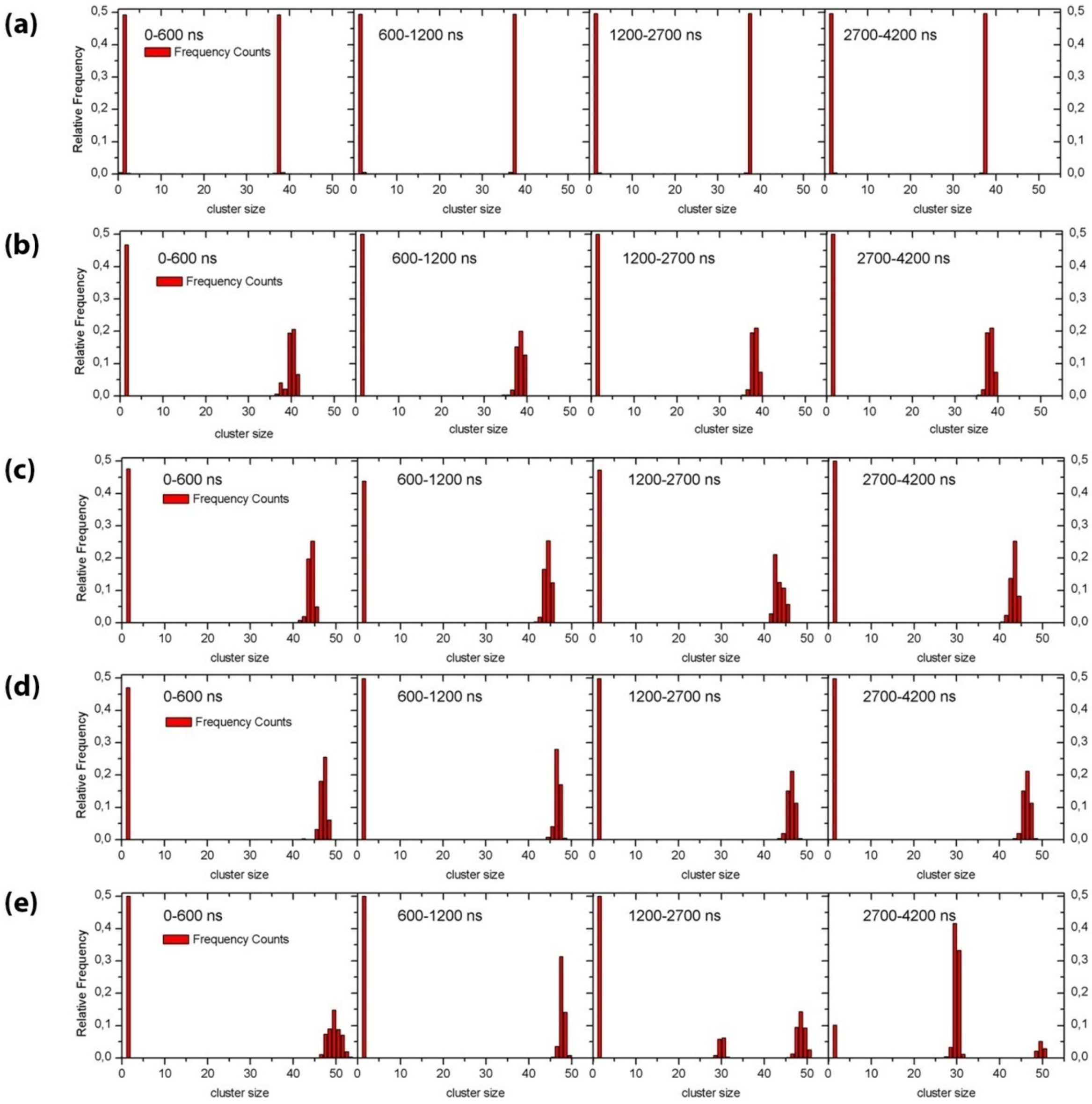

Figure S3 Frequency of occurrence of clusters of different size for systems a-e.

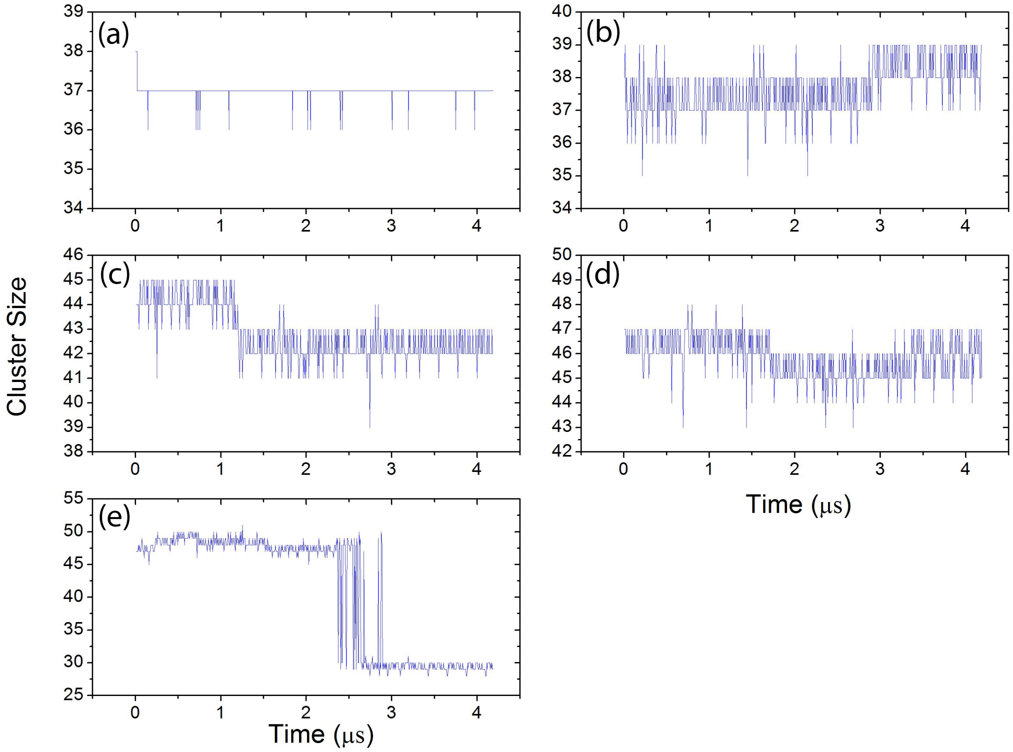

Figure S4 Time behavior of cluster size for the systems (a-e).

Validation of single trajectory behavior

In order to validate simulation results, three different independent simulations of the system III have been performed. In **Figure S5** block averages of three possible L64 chains states as function of time (inserted into bilayer, assembled and free; for a quantitative definition of these states the reader can refer to the caption of Figure 5 of the paper) are shown. The main behavior in all three cases is very similar and at equilibrium the chain distributions converge to similar values. Each point on the plot represents the time block average calculated using a time interval of 1.0 μs. In addition, in **Figure S6** the instantaneous time behavior of three independent simulations of the system III, jointly with average time behavior, is reported. From the **Figure S6** it is clear that the instantaneous behavior of a single simulation is representative of the whole process.

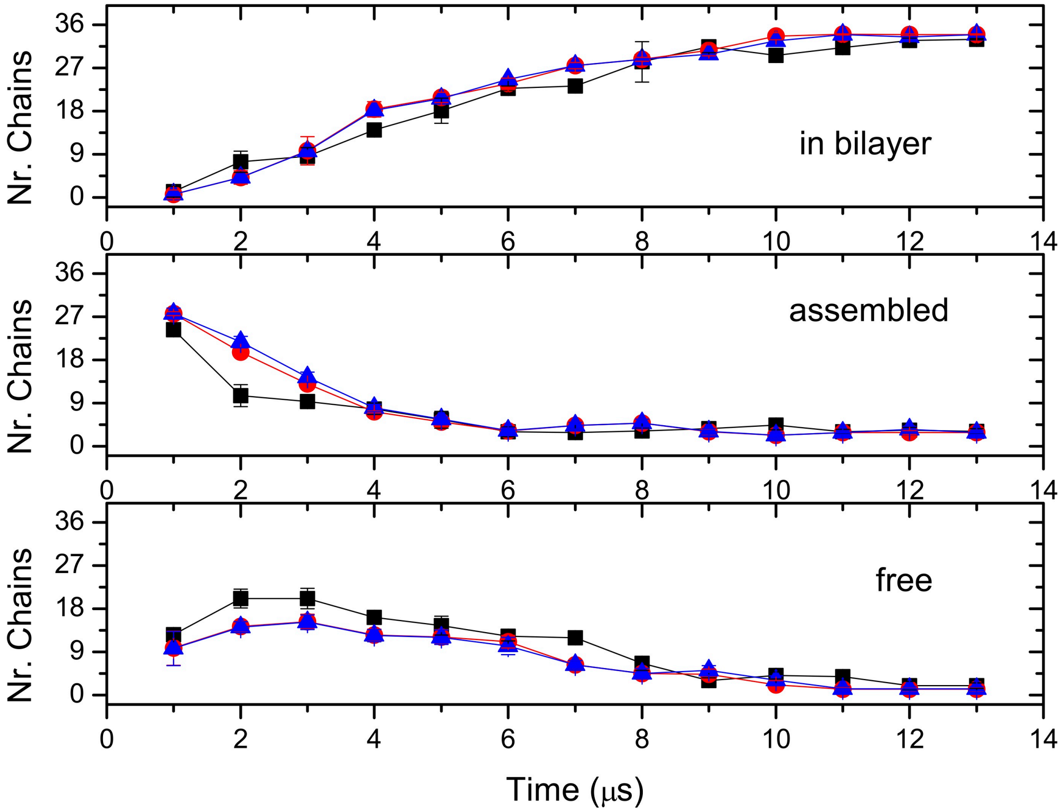

Figure S5 Time behavior of L64 chains in bilayer (top), assembled (middle) and free (bottom). Each point is a time average over 1.0 μs. Three different simulations of the system III have been used for the block average calculation (for the composition of the system III refer to table 6 of the paper).

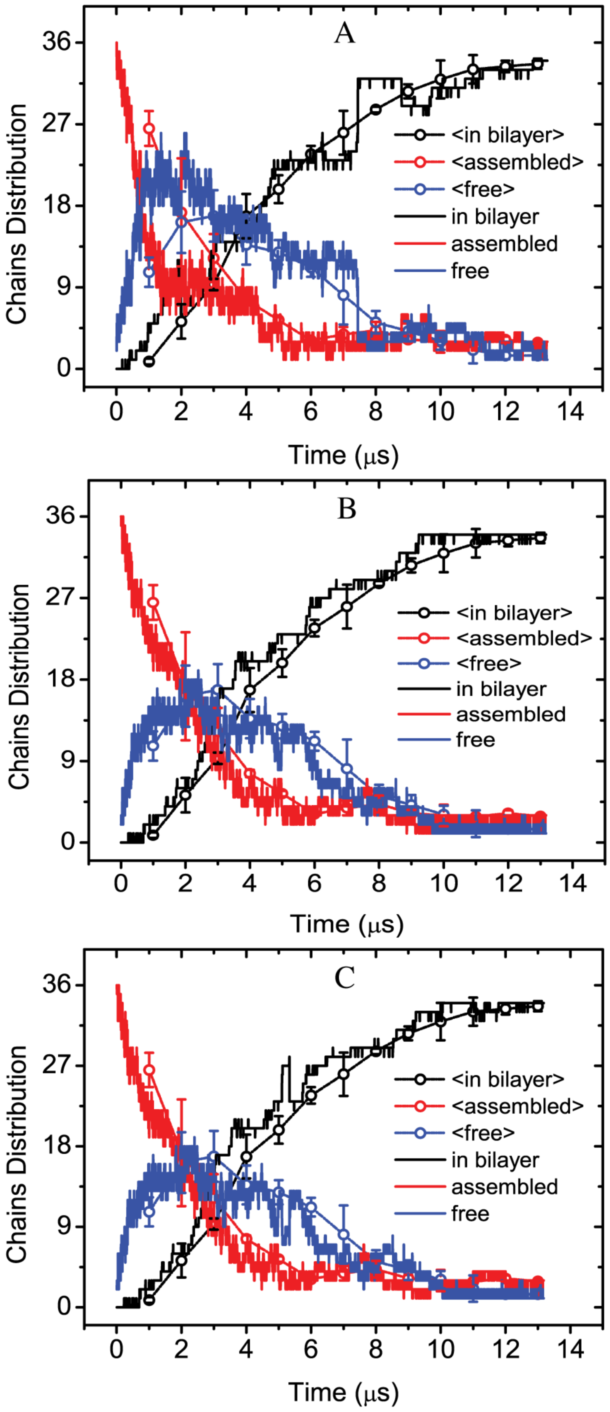
A
Chains Distribution
36
27
18
9
0
0
2
4
6
8
10
12
14
Time (μs)
<in bilayer>
<assembled>
<free>
in bilayer
assembled
free
B
Chains Distribution
Time (μs)
<in bilayer>
<assembled>
<free>
in bilayer
assembled
free
C
Chains Distribution
Time (μs)
<in bilayer>
<assembled>
<free>
in bilayer
assembled
free

Figure S6 Instantaneous behavior of three independent simulations (A,B,C) for the system III. The symbols represent the averages over 1.0 μs of each state of the chains (in bilayer, assembled and free).

The comparison between the equilibrium values of the micelle radius calculated using three independent simulations of the system III is repoted, jointly with the related table, below.

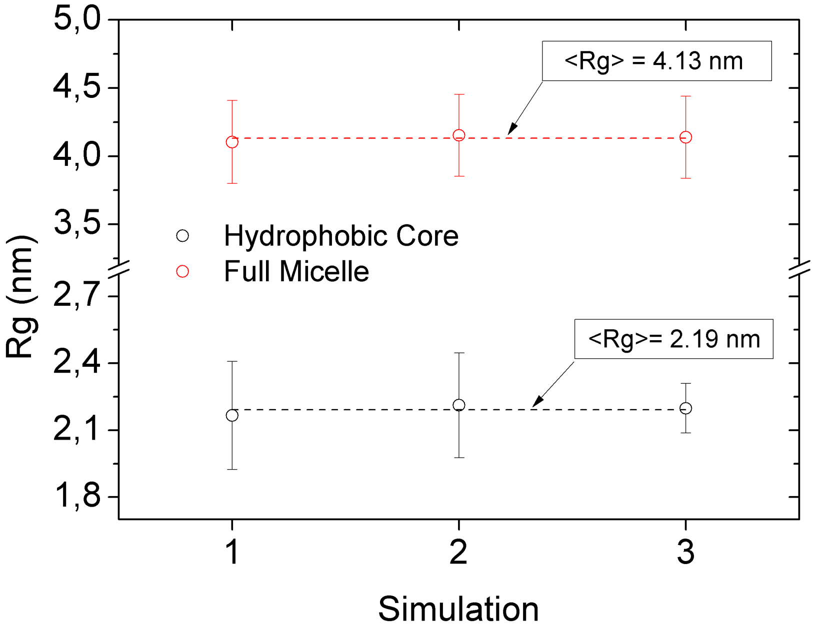

Figure S7 Radii of gyration of the hydrophobic core and full micelle calculated for three different simulation of the system III. Each point represent the time average over the last 1.0 μs of the each simulation.

Table 5 Radii of gyration calculated for three different simulation of the system III

Simulation	**Radius of gyration** (nm)			
	Hydrophobic Core	Standard Deviation %	Full Micelle	Standard Deviation %
1	2.17	6.3	4.10	8.0
2	2.21	6.1	4.15	7.9
3	2.20	2.9	4.14	7.9

Timescale Connection

Ideally, the exchange process of L64 chains between the micelle and the lipid bilayer, as discussed in the paper, can be divided in three elementary processes. In particular, we can consider three processes: Pluronic chain detachment from the micelle, chain diffusion in water, and chain insertion into the lipid bilayer. Reasonably, the diffusion process is the slowest and the governing the rate of the observed process. To better evaluate the time scales involved in such global process, a more systematic study has been done.

We performed three independent simulations similar to the one reported in Figure 6 of the main paper. In particular, we evaluated the velocity of L64 chain insertion in the following way. The time behavior of z component (perpendicular to the bilayer plane) of the distance between the geometrical center of the PPO block and the center of mass of the particles of type C (hydrophobic sector of the lipid bilayer) has been considered. In the figure below, the time behavior of this distance is reported. In order to estimate the velocity of this process the time behavior has been fitted with a sigmoidal function of the type:

$$z(t) = \frac{z_1 - z_2}{1 + e^{(t-t_0)/\delta t}} + z_2$$

The velocity of insertion can be estimated by considering the value of the first derivative at t_0 $z'(t_0) = \frac{z_2 - z_1}{4\delta t}$ as indicated in the figure below.

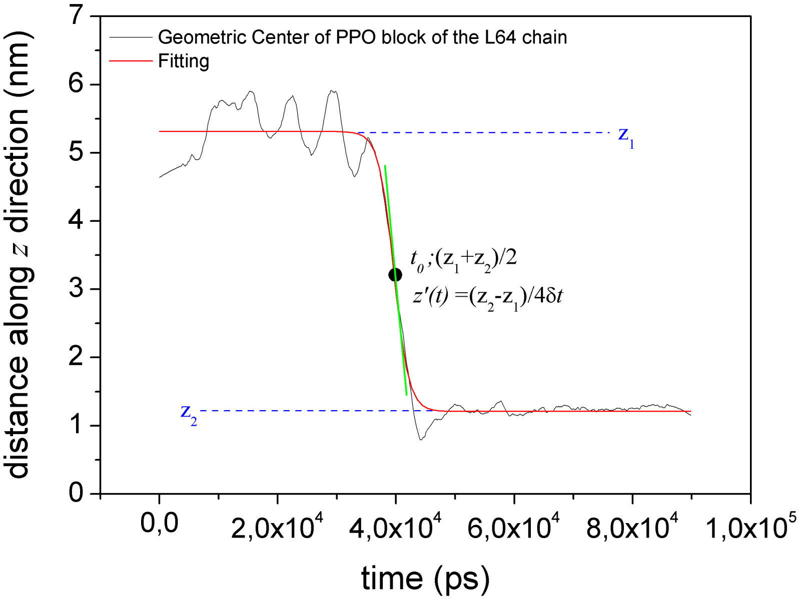

Figure S8 Time behavior of z component of the distance between geometric center of PPO block and center of mass of hydrophobic sector of the lipid bilayer during the insertion process of a single L64 chain (black curve). In red is reported the fitting obtained using a sigmoidal function defined with the equation above.

In the Table 6 the fitted velocities for three independent particle-particle and particle-field simulations are reported.

Table 6 Estimated insertion velocities for particle-particle and particle-field simulations

Simulation	(Particle-Particle) [nm/ps] 10^4	(Particle-Field) [nm/ps] 10^4
1	1.7 ± 0.2	2.9 ± 0.2
2	7.8 ± 0.3	2.6 ± 0.3
3	5.5 ± 0.4	5.6 ± 0.3

From the values reported in the table above it is clear that the process of chain insertion is fast (takes about 8-10 ns) and it has similar velocities for both particle-particle and particle field simulations.

According to these results we can reasonably conclude that the slowest process governing the chain exchange process between the micelle and the bilayer is the diffusion of L64 chains. In this way a reasonable estimate of the scaling factor could be the ratio between diffusion coefficients of particle-particle and particle-field simulations (a factor 15).

The time behavior of chain distribution of the systems IV-(A,C) are reported in **Figure S9**. For the composition of such systems refer to table 6 of the paper.

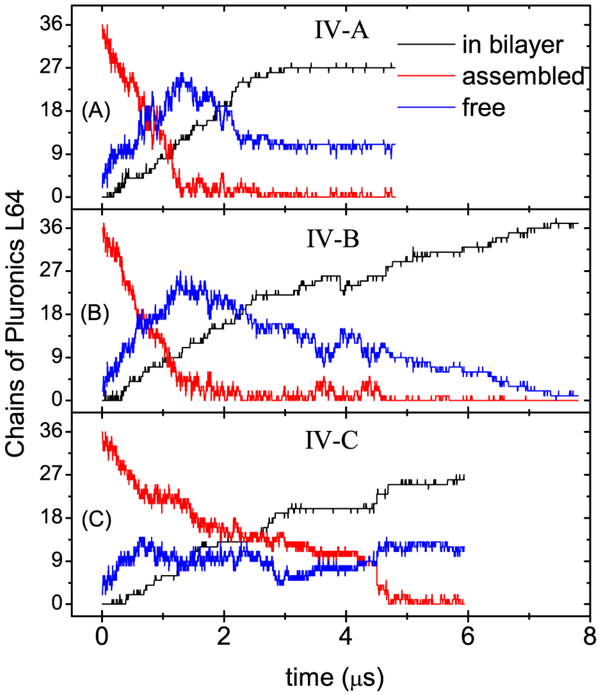

Figure S9 Time behaviour for systems IV-A,C (corresponding to systems with λ 0.16, 0.20 and 0.5) of L64 chains assembled as micelle (red curve), inside bilayer (black), in water (blue). The L64 chains, for a given configuration, are counted as inside bilayer if the last one PO bead is located between the average heighest of upper and lower lipid layers. The remaning chains are counted as free or assembled according to the number of neighboring chains (zero neighboring are considered free chains). The number of neighbors is calculated on the basis of a cut off criteria (1 nm) on the shortest distance between PO units of two different L64 chains.

The number density profiles of systems IV-(D-E-F) are reported in **Figure S10**. The last 0.5 μs of the equilibrium state of each simulation have been considered in the calculation of profiles.

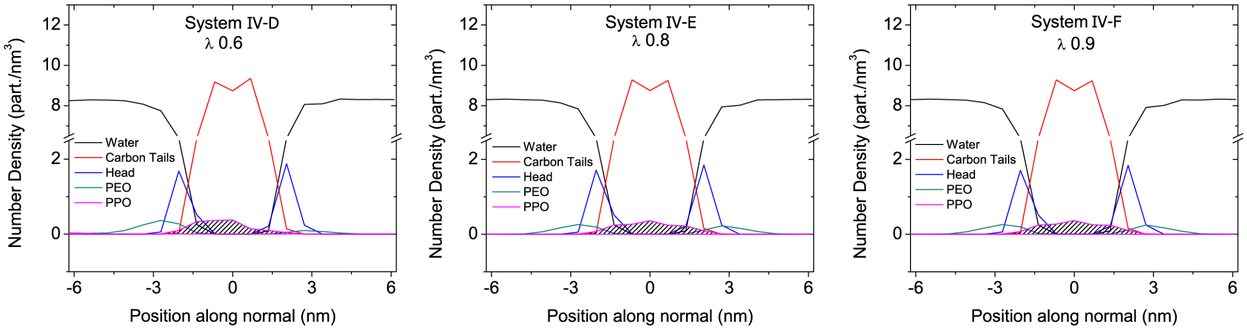

Figure S10 Number density profile of the systems IV-(D-E-F). We consider as lipid head the group of CG beads formed by N, P and g type. The carbon tails are counted as a single group of type C particles. For the particles type definition refer to the Figure 2 of the paper.

References

1. R. D. Groot and P. B. Warren, *The Journal of Chemical Physics*, 1997, **107**, 4423-4435.

2. S. Hezaveh, S. Samanta, G. Milano and D. Roccatano, *J. Chem. Phys.*, 2011, **135**, 16450.

3. P. Alexandridis, J. F. Holzwarth and T. A. Hatton, *Macromolecules*, 1994, **27**, 2414-2425

4. L. Yang, P. Alexandridis, D. C. Steytler, M. J. Kositza and J. F. Holzwarth, *Langmuir*, 2000, **16**, 8555-8561.